Catena 214 (2022) 106256

Contents lists available at ScienceDirect

Catena

journal homepage: www.elsevier.com/locate/catena

Mapping rainfall erosivity over India using multiple precipitation datasets

Ravi Raj [a], Manabendra Saharia [a,*], Sumedha Chakma [a], Arezoo Rafieinasab [b]

[a] Indian Institute of Technology Delhi, Hauz Khas, New Delhi 110016, India
[b] Research Applications Lab, National Center for Atmospheric Research (NCAR), United States

ARTICLE INFO

Keywords:
Rainfall erosivity factor
Modified Fournier Index
Rainfall-kinetic energy
Fournier Index
India

ABSTRACT

Rainfall erosivity is a measure of the erosive force of rainfall which represents the potential of rain to cause soil erosion. A large proportion of the total eroded soil in India is due to erosion by water, and rainfall erosivity is one of the major components. The current assessments of rainfall erosivity in India are however largely based on rain-gauge recordings and surveys which hinders its estimation and understanding over large areas. Growing availability of remotely-sensed gridded precipitation datasets presents an unprecedented opportunity to study long-term rainfall erosivity over varied terrains and address some of the limitations of point data-based estimations. In this study, multiple national and global gridded precipitation datasets were utilized to develop a high-resolution rainfall erosivity factor (R-factor) map to highlight areas prone to rainfall-induced erosion. Further, a large selection of empirical equations from literature were employed for estimating rainfall erosivity to provide a comparative analysis of these commonly adopted methods. The calculated rainfall erosivity is also compared with alternative methods to estimate R-factor such as Fournier Index (FI) and Modified Fournier Index (MFI). It was observed that MFI is highly correlated with rainfall erosivity, and an equation was finally proposed to estimate R-factor using MFI. This is the first such national-scale assessment of rainfall erosivity over India using gridded precipitation datasets, which will aid in understanding and mitigating rainfall-induced erosion.

1. Introduction

Soil erosion which is also called the 'creeping death of the soil' is a global problem (Tripathi and Singh, 1993). India is facing soil erosion problems in sectors such as reservoir siltation, soil-degradation and in agricultural sectors mainly. The upmost layer which is also the most fertile layer of the soil, is also most exposed to erosion induced by water (Lukić et al., 2019; 2018). Rainfall erosivity also known as rainfall-runoff erosivity factor is one of the contributing factors to the Universal Soil Loss Equation (USLE) (Wischmeier and Smith, 1978) as well as the Revised Universal Soil Loss Equation (RUSLE) (Renard et al., 1997), which is used to estimate long term average soil loss. This study performs a comprehensive estimation of rainfall erosivity over India as well as establishes new empirical equations suitable for field applications.

Apart from classical models such as USLE and RUSLE, several large-scale soil erosion models have also been used at continent level to estimate soil erosion (Bosco et al., 2015; Morar et al., 2021; Panagos et al., 2015b). Soil erosion models play a significant role in the planning and implementation of soil management strategies (Lukić et al., 2019; Panagos et al., 2015a). The potential ability of rainfall to erode soil is termed rainfall erosivity (Wischmeier, 1959), which is one of the best indicators (Renard et al., 1991) to measure the erosive potential of rainstorms for a particular duration. When a rainfall droplet falls on the soil surface it exhibits forces on the surface, and if the forces applied exceed the cohesive forces between the soil particles, the movement of soil particles start (Bryan, 2000). Studies highlighted rainfall erosivity as a key factor to investigate natural hazards such as landslides and floods as it is one of major root-causing reasons for these hazards (Capolongo et al., 2008; Diodato, 2004; Nazzareno et al., 2015). Ideally, the R-factor should be estimated using high-resolution with 1–5-minute interval precipitation

Abbreviations: FI, Fournier Index; MFI, Modified Fournier Index; USLE, Universal Soil Loss Equation; RUSLE, Revised Universal Soil Loss Equation; IMDAA, Indian Monsoon Data Assimilation and Analysis; IMD, India meteorological Department; CHIRPS, Climate Hazards Group InfraRed Precipitation with Station data; NCMRWF, National Centre for Medium Range Weather Forecasting; NMM, National Monsoon Mission; 4DVAR, Four-Dimensional Variational Assimilation Scheme; HadISST2, Hadley Centre Ice and Sea Surface Temperature dataset version 2; FEWS NET, Famine Early Warning Systems Network; TMPA 3B42, Tropical Rainfall Measuring Mission Multi-satellite Precipitation Analysis; TARCAT, TAMSAT African Rainfall Climatology And Time series; NOAA, National Oceanic and Atmospheric Administration; GPCC, Global Precipitation Climatology Centre.

* Corresponding author at: Indian Institute of Technology Delhi, Hauz Khas, New Delhi 110016, India.
E-mail address: msaharia@iitd.ac.in (M. Saharia).

https://doi.org/10.1016/j.catena.2022.106256
Received 24 May 2021; Received in revised form 22 March 2022; Accepted 26 March 2022
Available online 13 April 2022

records (Williams and Sheridan, 1991) but such datasets are not available in most parts of the world for long-enough periods. So, half-hourly or hourly data has been widely used for the estimation of the rainfall erosivity factor using the kinetic energy-rainfall intensity principle (Padulano et al., 2021; Panagos et al., 2017). The rainfall erosivity factor (Annual R-factor) is one of the factors of the widely adopted RUSLE (Revised Universal Soil Loss Equation) model, and calculated for a minimum period of 20 years as the average of the sum of the rainfall erosivity factors for every year (Vantas et al., 2019). Proper measurement of both rainfall intensity and kinetic energy is required to get an accurate estimation of the R-factor, but it is very difficult to record rainfall kinetic energy directly as the instruments required are costly, and the measurement of the drop size distribution of the rainstorm is an inconvenient method (Dash et al., 2019; Fornis et al., 2005). There are numerous mathematical empirical relationships (linear, polynomial, logarithmic, exponential, and power-law functions between rainfall intensity and kinetic-energy) to estimate the kinetic energy of a rainstorm (Rosewell, 1986). Dash et al. (2019) collated fourteen empirical equations to estimate kinetic energy developed by researchers across the world from which they used only six for their study because of their universal application (Dash et al., 2019), the same six equations were adopted in this study.

The R-factor is highly sensitive to the method used to estimate EI_{30} (R-factor for 30-minutes rainfall intensity) and the amount of I_{30} (30-minutes rainfall intensity) (Catari et al., 2011), but if I_{30} value records are not available, then other forms of intensity estimation are used (I_5, I_{10}, I_{15}, I_{40}, I_{60}) (Sharifah et al., 2006; Sinzot et al., 1989; Usón and Ramos, 2001). There are contradictory points of view on the selective use of these intensities (Zheng and Chen, 2015). In Eastern Ghats of India, Dash et al., (2019) and Rajbanshi and Bhattacharya (2020) emphasized that if we use hourly rainfall intensity data (I_{60}) instead of half hourly (I_{30}), it underestimates the value of the R-factor by 23.4% while Lobo and Bonilla (2015) pointed out in their study that the R factor estimated using I_{60} gives a value less than 10% as compared to that of I_{30}. The R-factor computation using I_{30} and I_{60} rainfall data are also known as EI_{30} and $EI_{60,}$ respectively. In this study, I60 will be considered as I30 due to inaccessibility of sub-hourly data at national scale. 3-hourly precipitation product (TMPA 3B42) has been used to estimate rainfall erosivity factor for Africa (Vrieling et al., 2010). They had used 3 hourly rainfall value as the value of I30, although I30 would be higher than the mean precipitation intensity during 3 h (Vrieling et al., 2010).

Spatial variation in the R-factor is not certain in comparison with the spatial variation of rainfall as it occurs in Indian conditions (Tiwari et al., 2016). The R-factor can also be computed using indices such as Fournier Index (FI) and Modified Fournier Index (MFI) when high-resolution precipitation datasets are unavailable (Pandey et al., 2007; Prasannakumar et al., 2011). MFI has been used to assess rainfall erosivity and its relationship with other climatic variables which lead to estimate disastrous erosion (Lukić et al., 2016; Morar et al., 2021). All the studies performed in the Indian context thus far have been based on gauge-based precipitation records. The average annual R-factor for Kerala state was computed as 151.466 MJ cm/ha/h/yr for years 2004–2008 (Prasannakumar et al., 2012), but variation in the R-factor was reported at the nearby locations in the same state as 3.16 MJ cm/ha/h/yr for the years 2005–2008 (Prasannakumar et al., 2011). In Arunachal Pradesh also such type of variation was reported. Dabral et al., (2008) considered average annual R-factor for the state as 189.46 MJ cm/ha/h/yr, but Rawat et al., (2013) experimentally estimated the annual R-factor as 974.77 MJ cm/ha/h/yr with standard deviation of 160.16 MJ cm/ha/h/yr.

Theoretically, Tiwari et al., (2016) estimated the R-factor for 52 gauge stations and later interpolated over whole India. Dash et al., (2019) also mapped rainfall erosivity for Eastern Ghats of India using gauge-based precipitation and the annual R-factor varied from 3040 to 10127 MJ-mm/ha/h/yr with standard deviation of 1981 MJ-mm//ha/h/yr. A global R-factor map was created by Panagos et al., (2017) covering a total of 87 countries of the globe considering high resolution datasets of 1675 rainfall stations. They also mapped the R-factor for India considering hourly rainfall dataset of 247-gauge stations for an average seven years (2007–2015) and interpolated the results to get the rainfall erosivity map at 30 arc seconds (~1km).

In this study, for the first time, multiple gridded precipitation datasets were used to calculate rainfall erosivity over India. The R-factor was calculated for a minimum period of 20 years to counter the uncertainties and biasness raised due to wet and dry seasons (Vantas et al., 2019). Although gauge-based rainfall provides accurate records of the occurred precipitation, it has limitations due to poor spatial coverage in many parts of the globe (Kidd and Huffman, 2011; New et al., 2001), and gauge data alone are not sufficient to for many hydrologic simulations (Kotlarski et al., 2019; Villarini and Krajewski, 2008). Gridded precipitation has its own limitations depending upon the source and mode of the derivation of the data and also due to the intrinsic differences in spatial scales (Chen et al., 2008; Shen et al., 2010; Tapiador et al., 2012; Xie et al., 2007).

The objectives of this study were to create a R-factor map for India using high resolution gridded precipitation data, highlighting the rainfall-erosivity-prone areas and analyzing the sensitivity of the method chosen to estimate rainfall erosivity over India. This will be the first such national-scale assessment of rainfall erosivity over India using gridded precipitation. Agricultural experts as well as soil conservational experts could apply the rainfall erosivity map to incorporate safety measures to minimize soil erosion.

2. Material and methodology

2.1. Study area

Our study covers the entire political boundary of India. India is the seventh-largest country in the world and is surrounded by three major oceans - Arabian Sea, by the Indian Ocean, and the Bay of Bengal. Its diverse climatic conditions range from deserts in the west, glaciers in the north, humid tropical forests in the southwest, and many islands in the Arabian Sea and the Bay of Bengal. The nation's tropical climate is classified into four main seasons i.e., monsoon, post-monsoon, summer, and winter as per the India Meteorological Department (IMD). The Ganga and Brahmaputra delta covers most of the middle, northern, and eastern parts of the country while the southern part is covered by the Deccan Plateau. Indian climate is dominated by the monsoons which is transited to wetter regimes from drier regimes. The average precipitation recorded in the southwest monsoon (June to September) is 877.2 mm, which is almost 74% of the annual precipitation i.e., 1182.8 mm (Singhvi, 2014). The distribution and intensity of the monsoon rainfall has been highly variable in spatial and temporal aspects. It has been reported that a 20–30% variation from the mean rainfall leads to hazards such as droughts and floods in the Indian subcontinent (Singhvi, 2014). The lowest and highest average yearly rainfall was recorded at Jaisalmer (130 mm) and Mawsynrum (near Cherrapunji, 11410 mm) respectively considering data from 1870 to 2010 (Singhvi, 2014). Rainfall erosivity which is solely derived from the rainfall intensity datasets, and rainfall pattern is directly related to these climatic properties. Since Indian climate is diverse in nature, and climate change has been spotted nationwide in the past decades, a relatively longer duration rainfall period should be incorporated to estimate R-factor. Climatic properties have adversely affected the rainfall pattern throughout the nation. So, a relatively longer duration rainfall datasets have been used (greater than20 years) to counter the uncertainties and biasness raised due to change in climatic properties especially due to wet and dry seasons as suggested by Vantas et al., (2019).

Table 1
The selected gridded datasets to estimate rainfall erosivity factor over India with their specifications.

Product	Full Name	Spatial Resolution	Temporal Resolution	Time period	Format	Providing Agency
IMD Gridded daily	Indian Metrological Department Long-term Daily Gridded Precipitation	0.25° x 0.25°	1-day	1901–01-01 to 2019–12-31	netcdf	IMD, Ministry of Earth Sciences Govt of India
CHIRPS-2.0 Global_daily	Climate Hazards Group InfraRed Precipitation with Station data	0.05° x 0.05°	1-day	1981–01-01 to 2019–12-31	netcdf	UC SANTA BARBARA Climate Hazards Center
IMDAA 1-Hourly	The Indian Monsoon Data Assimilation and Analysis reanalysis	0.12° x 0.12°	1-hour	1979–01-01 to 2018–12-31	netcdf	NCMRWF, Ministry of Earth Sciences Govt of India

2.2. Data acquisition and preparation

For mapping of the R-factor over India, gridded datasets were used. Three sets of gridded precipitation datasets were utilized for this study -.

a) Hourly IMDAA (Indian Monsoon Data Assimilation and Analysis).

b) Daily IMD (India meteorological Department).

c) Daily CHIRPS (Climate Hazards Group InfraRed Precipitation with Station data).

The IMD daily gridded precipitation is a rain-gauge-derived product (Pai et al., 2014), CHIRPS daily is a satellite-gauge merged product (Funk et al., 2015), and IMDAA hourly is a reanalysis product derived from historical rain-gauge station datasets (Indirarani et al., 2021). These three datasets were used in the current study to cover the mode and source of derivation of different gridded precipitation products and its relationship with rainfall erosivity in the Indian context. The specifications of the gridded datasets used for rainfall erosivity estimation are listed in Table 1.

2.2.1. IMDAA hourly

The association of National Centre for Medium Range Weather Forecasting (NCMRWF), India, Met Office, UK, and the India Meteorological Department (IMD) for the National Monsoon Mission (NMM) have launched a high spatio-temporal resolution historical data assimilation product i.e., IMDAA (The Indian Monsoon Data Assimilation and Analysis) (Indirarani et al., 2021) having 12 km spatial and 1 h temporal resolution for 40 years (1979–2018) for the National Monsoon Mission (NMM) funded by the Ministry of Earth sciences, Government of India.

The IMDAA system is based on the Met Office four-dimensional variational assimilation scheme (4DVAR) (Rawlins et al., 2007) and its Unified Model (Davies et al., 2005). To cover the areas necessary for the development of Indian Monsoon, the domain of the model is extended wider than the Indian subcontinent. The system uses a 6-hour intermittent DA cycle. Horizontal resolution of the model is approximately 12 km while 63 vertical levels are reaching to a height of about 40 km. This model takes global reanalysis ERA-Interim as lateral boundary conditions for the reanalysis run and sea surface temperature is incorporated from the Hadley Centre Ice and Sea Surface Temperature dataset version 2 (HadISST2) (Titchner and Rayner, 2014). In this study IMDAA hourly data will be used as I_{60} i.e., hourly rainfall intensity for the estimation of rainfall erosivity factor as well as FI and MFI indices.

2.2.2. CHIRPS daily

Climate Hazards Center University of California, Santa Barbara launched CHIRPS (Climate Hazards Group InfraRed Precipitation with Station data) version 2.0 final gridded daily data having 0.05-degree spatial resolution. 39 years (1981–2019). CHIRPS was developed to support the International Development Famine Early Warning Systems Network (FEWS NET) by the United States Agency (Funk et al., 2015). CHIRPS data was built using the Tropical Rainfall Measuring Mission Multi-satellite Precipitation Analysis version 7 (TMPA 3B42 v7)

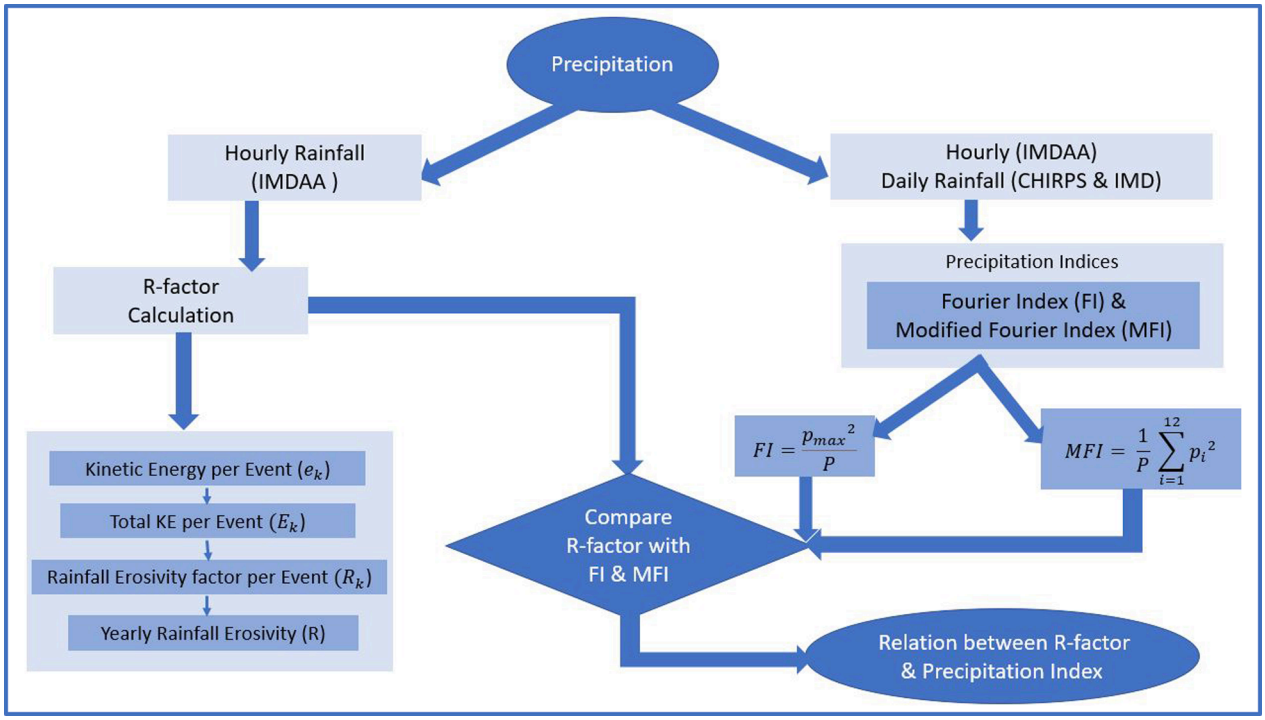

Fig. 1. Methodology for computing rainfall erosivity.

(Huffman et al., 2007) which was based on the approaches used in thermal infrared (TIR) precipitation products like African Rainfall Climatology or the University of Reading's TAMSAT African Rainfall Climatology And Time series (TARCAT) (Abram et al., 2008; Maidment et al., 2014; Tarnavsky et al., 2014), National Oceanic and Atmospheric Administration's (NOAA's) Rainfall Estimate (RFE2) (Love et al., 2004; Xie and Arkin, 1997), to calibrate global Cold Cloud Duration (CCD) rainfall estimates. CHIRPS also used a 'smart interpolation' technique built on the approaches incorporated in current state-of-the-science interpolated gauge products (Becker et al., 2013; Harris et al., 2014; New et al., 1999; Schneider et al., 2014; Willmott and Matsuura, 2009).

CHIRPS lies somewhere in between merged-gauge-satellite precipitation product (RFE2) and highly interpolated rain-gauge based product (Global Precipitation Climatology Centre, GPCC)(Becker et al., 2013; Schneider et al., 2014; Willmott and Matsuura, 1995; Willmott and Robeson, 1995). CHIRPS assimilates station data in a two-phase process, yielding two unique products. CHIRPS daily dataset was used for the current research work because it blended gauge-satellite precipitation estimates that capture the whole world regions with fairly low latency, low bias, high resolution and for longer span of time (Funk et al., 2015). CHIRPS daily data will be used to calculate the FI (Fournier Index) (Fournier, 1960) and MFI (Modified Fournier Index) (Arnoldus, 1977) over the study region.

2.2.3. IMD daily

IMD (Indian Metrological Department) has compiled and interpolated the historical precipitation datasets to create a 0.25-degree high resolution gridded precipitation for 119 years (1901–2019) over India, which is used in the current study. Data was distributed over the country in 135x129 grid points. The first gridded precipitation at daily scale having 1°spatial resolution over Indian region was prepared by Hartmann and Michelsen, (1989). (Hartmann and Michelsen, 1989; Krishnamurthy and Shukla (2008, 2007, 2000) analyzed this gridded dataset to study the interannual and the intra-seasonal variability of precipitation over India. IMD produced a high spatial resolution (~25 km) daily rainfall dataset for 110 years (1901–2010) over India considering all the available quality rain-gauge data throughout the nation (Pai et al., 2014). IMD daily data will be used to estimate the FI and MFI indices over India.

2.3. Methodology

Two approaches were adopted for mapping the R-factor over India as illustrated in Fig. 1. In the first approach, rainfall erosivity was calculated using high resolution gridded precipitation (I60) with the concept that the product of total kinetic energy of a storm to its hourly (hourly maximum) rainfall intensity (KE × I60) is expressed as rainfall erosivity (R-factor). In the second one, Fournier Index (FI) and Modified Fournier Index (MFI) were calculated using daily (IMD and CHIRPS) precipitation datasets. These indices were calculated individually and then analyzed with the yearly average rainfall erosivity values to check for better correlation with R-factor values. Several studies in the past (Tiwari et al., 2016; Vrieling et al., 2010) have suggested empirical equations to estimate yearly rainfall erosivity with the help of precipitation indices such as MFI (Tiwari et al., 2016; Vrieling et al., 2010). In this study, a new empirical equation was proposed for the estimation of average rainfall erosivity using Modified Fournier index as it was highly correlated (Pearson correlation 0.83) with the R-factor. Since, IMD has divided whole India into four regions depending upon the climate conditions, additional equations were derived for each IMD region. ArcMap 10.5 and Python/Jupyter notebooks were utilized for computation and visualization.

2.3.1. R-factor computation

In this approach, the rainfall erosivity factor was computed using standard equations mentioned by (Wischmeier and Smith, 1978) and in the RUSLE user guide (Renard et al., 1994). The R-factor is set equal to the average of the summation of the erosivity values for every year's rainfall and defined by the product of an erosive rainfall event's kinetic energy and the maximum intensity of a 30-minute duration rainfall, during the rainfall event, known as EI_{30}. In this study, EI_{60} was used instead of EI_{30} due to inaccessibility of sub-hourly data at national scale.

Table 2
List of empirical equations for the computation of kinetic energy corresponding to the rainfall event with their references.

Equation	References	Equation No.
$e_k = 0.119 + 0.0873\log(i), i \le 76 e_k = 0283, i > 76$	(Wischmeier and Smith, 1958)	1
$e_k = 0, i \le 4 e_k = 0.2986(1 - 4.29(i)^{-1}), i > 76$	(Hudson, 1961)	2
$e_k = 0.29[1 - 0.72e^{-0.05(i)}]$	(Brown and Foster, 1987)	3
$e_k = 0.29[1 - 0.72e^{-0.082(i)}]$	(McGregor et al., 1995)	4
$e_k = 0.283[1 - 0.52e^{-0.042(i)}]$	(Van Dijk et al., 2002)	5
$e_k = 0.1418(i)^{0.172}$	(Meshesha et al., 2016)	6

First of all, rainfall kinetic energy for each rainfall event was calculated using six empirical equations recommended by Dash et al., (2018) due to their global applicability, the details of which are provided in Table 2, where I is rainfall intensity and e_k is the kinetic energy of the event. Using all the six equations (1 to 6) kinetic energy (e_k) in MJ/ha/mm was calculated corresponding to the rainfall intensity (i) in mm/h.

In the next step, total kinetic energy (E_k) per erosive event in MJ/ha was estimated by multiplying the kinetic energy per event e_k with the precipitation amount (pk) in mm captured in that duration using equation (7).

$$E_k = e_k{}^* p_k = e_k{}^*(i) \tag{7}$$

After that, the rainfall erosivity factor (R_k) per erosive rainfall event was calculated by multiplying E_k with the corresponding I_{60} value. In this study, I60 (hourly) (in mm/h) rainfall intensity values were used to calculate EI_{60} as R-factor in MJ-mm/ha/h which is shown in equation (8).

$$R_k = EI_{60} = E_k{}^* I_{60} \tag{8}$$

Yearly rainfall erosivity (R) in MJ-mm/ha/h/yr value were then determined using equation (9), where n is the number of years for a particular dataset, here 40 years for EI_{60}, and m is the number of erosive events during year j.

$$R = \frac{1}{n}\sum_{j=1}^{n}\sum_{k=1}^{m} R_k \tag{9}$$

Intercorrelation analysis has been done among these R-factor maps. A rectangular distribution of points with 0.044° arc-distance (~5 km) incremental in both latitude and longitude covering national boundary from (6.84° N, 68.28° E) to (36.96° N, 98.40° E) was prepared and the values of R-factors were extracted for those points from the calculated maps. These extracted values of R-factors were intercorrelated using Pearson's correlation coefficient to get the values of correlation coefficients.

2.3.2. FI and MFI estimation

In the second approach, two commonly used indices (Fournier index, FI and Modified Fournier Index, MFI) to estimate rainfall erosivity factor were used. Daily gridded (IMD and CHIRPS daily) precipitation data were analyzed to calculate these indices. Fournier featured an index for the computation of the aggressivity of rainfall to degrade soil, which is known as Fournier index (FI) (FAO, 1977). It is defined as the proportion of the square of the wettest month rainfall to the total rainfall of the year for a given location, which is mentioned in equation (10).

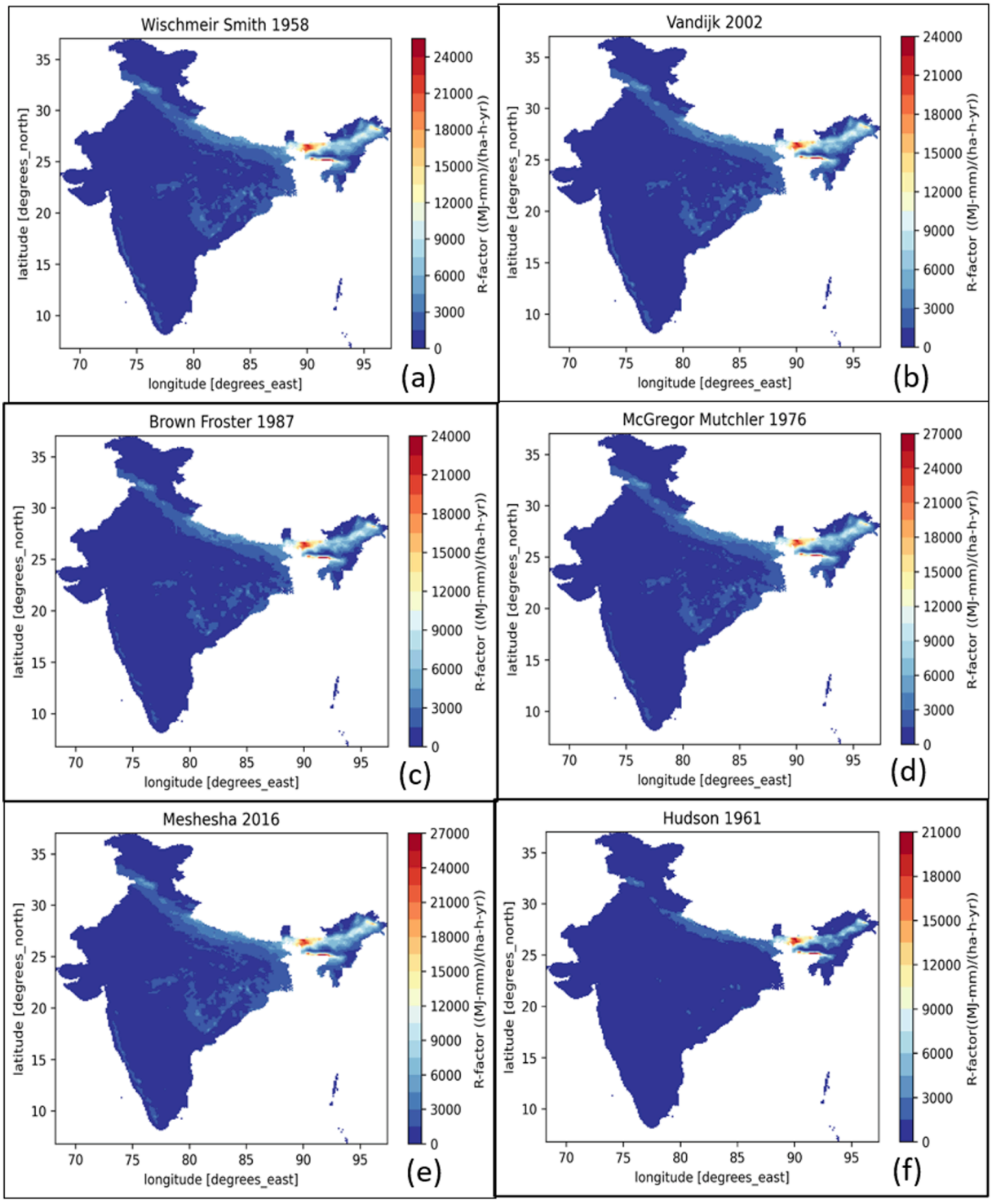

Fig. 2. (a) to 2(f) Rainfall erosivity (R-factor) maps for India using (Wischmeier and Smith, 1958), (Van Dijk et al., 2002), (Brown and Foster, 1987), (McGregor et al., 1995), and (Meshesha et al., 2016), (Hudson, 1961) based equations respectively.

$$FI = \frac{{p_{max}}^2}{P} \tag{10}$$

where p_{max} is the wettest month and P is the total precipitation of the year.

Modified Fournier Index (MFI) (Renard and Freimund, 1994) is defined as the summation of the monthly rainfall to its annual rainfall for a year and shown in equation (11).

$$MFI = \frac{1}{P}\sum_{i=1}^{12} {p_i}^2 \tag{11}$$

where p_i is the monthly precipitation (mm) in month i and P is the yearly precipitation.

Analyzing and inter-correlating all the six kinetic energy R-factors using I60 (hourly rainfall intensity) dataset, one R-factor map for India was selected considering the magnitude of Person's correlation

Table 3
Average R-factor for Region defined by IMD.

IMD Regions	Average R-factor (MJ-mm/ha/h/yr)
Central India	881.74
East and North East India	3312.39
North West India	834.44
South Peninsula	615.61

coefficient. These R-factor maps were further compared with FI, MFI, and average yearly precipitation values to get relationships with the erosivity factor in the Indian context.

FI (Fournier Index) and MFI (Modified Fournier Index) were calculated using IMD and CHIRPS daily precipitation and using IMDAA hourly precipitation datasets with the help of equations (10) and (11), respectively. These indices are calculated using python with the help of its libraries as an average period of 119, 39 and 40 years, respectively for IMD daily, CHIRPS daily and IMDAA hourly precipitation data.

3. Results and discussions

3.1. R-factor estimation

IMDAA hourly (I_{60}) precipitation data was used to estimate rainfall erosivity factor using all the six equations (equations 1 to 6) of kinetic energy-based methods explained in the previous section. The average R-factor averaged over 40 years are shown in Fig. 2(a) to 2(f).

The R-factors estimated using all the six equations exhibit a similar trend and spatial distribution throughout the nation (Fig. 2(a) to 2(f)). The regions having higher values of R-factor, i.e., regions prone to rainfall-induced erosion, are Assam and Meghalaya sub-division and some parts of north-eastern Himalayan belt & along the Eastern Ghat of the country. East and Northeast India rainfall region, as defined by IMD, have the highest average R-factor value (3312.39 MJ-mm/ha/h/yr) while the southern Peninsula region (615.61 MJ-mm/ha/h/yr) is least prone to rainfall erosivity (Table 3).

Calculated Pearson correlation coefficients are shown in Fig. 3. From the heatmap shown in Fig. 3, all the methods are well correlated having more than 0.98 correlation value except R-factor estimated using Hudson (equation 2) method. It implies that any method among these six could be used in the Indian context for rainfall erosivity estimation. In this study, Equation 5 (Van Dijk et al., 2002) was incorporated for further analysis. The average R-factor value estimated for India is 1200 MJ-mm/ha/ha/yr, while maximum rainfall erosivity value 23909.21 MJ-mm/ha/h/yr was spotted in the Laitknsew and Cherrapunji region of East Khasi Hills in Meghalaya state, and minimum value of 8.10 MJ-mm/ha/h/yr in the Shahi Kangri mountain region of Ladakh area.

A global R-factor map was prepared by (Panagos et al., 2017) with 30 arc-seconds spatial resolution available for download in the European Soil Data Centre (ESDAC) (Panagos et al., 2015a) website at https://esdac.jrc.ec.europa.eu. For India it was downloaded and analyzed. It was observed that there was variation in R-values estimated, 3848.97 MJ-mm/ha/h/yr as average R-factor and 12749 MJ-mm/ha/h/yr as maximum R-value. To check spatial correlation of the calculated R-factor with Panagos et al., (2017) study, a total of 1153 values were extracted and compared by creating (0.12° * 0.12°) grid points throughout the country (Fig. 9) with Pearson correlation 0.74. This difference could be due to the source of estimation of rainfall erosivity factor, and the duration of the rainfall captured in the study. Because Panagos et al., (2017) used the gauge-based hourly precipitation data for an average of seven years (2007–2015) for 247 rain gauge-stations only while in this study IMDAA gridded precipitation having (0.12°X0.12°) spatial resolution was used for time period of 40 years (1979–2018) over India. For example, Vantas et al., (2019) states that the R-factor should be calculated for a minimum of twenty years to counter biasness raised by wet and dry seasons. So, this study is more comprehensive as it accounts for forty years of data and thereby will provide improved R-factor values in the Indian context.

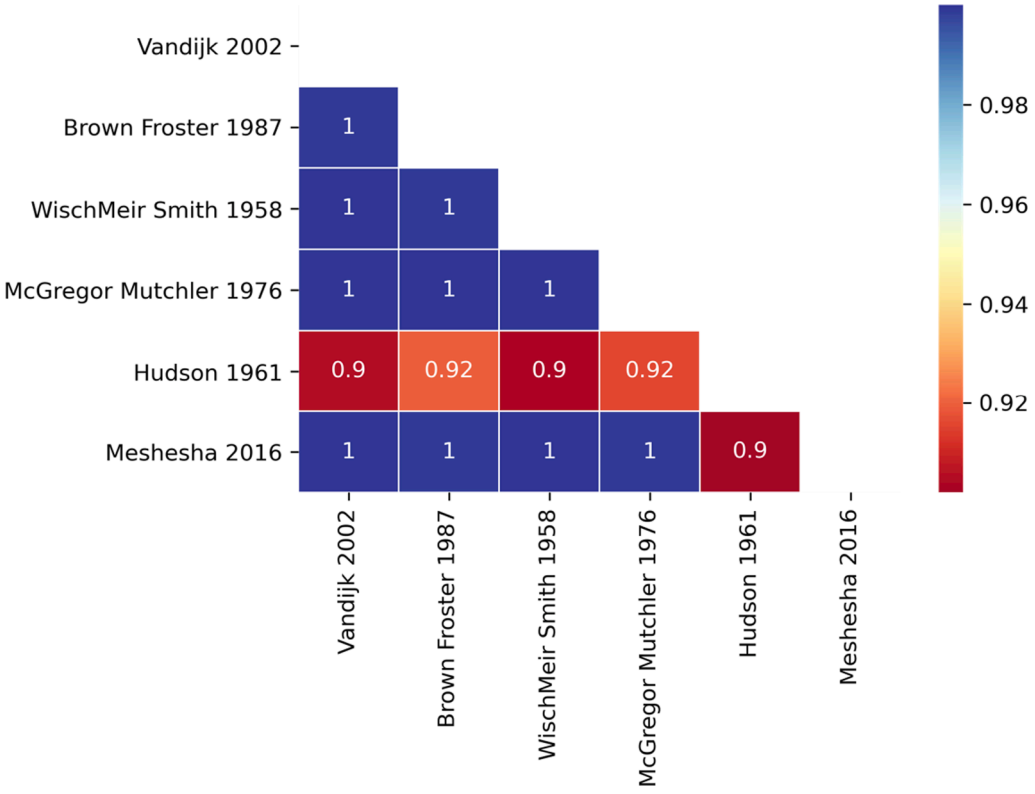

Fig. 3. Intercorrelation of R-factor maps using (Wischmeier and Smith, 1958), (Van Dijk et al., 2002), (Brown and Foster, 1987), (McGregor et al., 1995), and (Meshesha et al., 2016), (Hudson, 1961) based equations respectively.

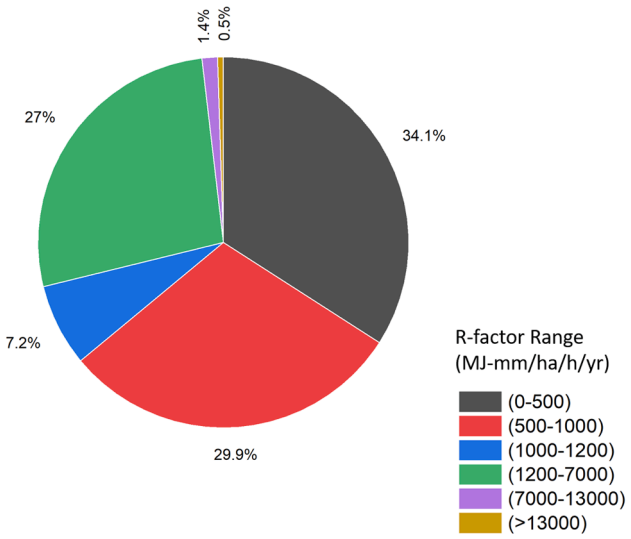

Fig. 4. A pie-chart showing the distribution of total point stations taken, grouped with the cumulative percentage of R-factor values.

R-factor values were further grouped in a way to visualize the distribution of rainfall erosivity (Fig. 4). About 71.2% of the total point values taken into analysis are less than average value of R-factor (1200 MJ-mm/ha/h/yr). Around 34.1% of total point samples had values less than 500 MJ-mm/ha/h/yr and 64% samples had values less than 1000 MJ-mm/ha/h/yr. Only 1.95% R-values estimated were greater than 7000 MJ-mm/ha/h/yr and 0.5% values greater than 13000 MJ-mm/ha/h/yr.

An analysis was also performed in the sub-divisions defined by IMD to visualize the spatial variation of the rainfall erosivity factor across the nation (Fig. 5(a) and 5(b)). The distribution of average R-factor at sub-division level is shown in Fig. 5(a). Assam & Meghalaya sub-division has the highest average R-factor value (7643.09 MJ-mm/ha/h/yr) while Jammu and Kashmir have the lowest (318 MJ-mm/ha/h/yr). Out of 36 sub-divisions defined by IMD only 13 (Arunachal Pradesh, Assam & Meghalaya, Bihar, Chhattisgarh, Himachal Pradesh, Jharkhand, NMMT, Orrisa, East Uttar Pradesh, West Uttar Pradesh, Uttarakhand, Gangetic West Bengal, and SHWB & Sikkim sub-divisions) have average R-factor values greater than national average rainfall erosivity value (1200 MJ-mm/ha/h/yr). The minimum of temporal average minimum rainfall erosivity value (8.10 MJ-mm/ha/h/yr) was recorded in Jammu and Kashmir sub-division while maximum of temporal average R-factor value was spotted in Assam and Meghalaya sub-division. Only, Assam &Meghalaya sub-division is there having average rainfall erosivity factor greater than 6000 MJ-mm/ha/h/yr.

District-wise average rainfall erosivity was also shown in Fig. 5(b). Kokrajhar district of Assam & Meghalaya sub-division is more vulnerable to rainfall erosivity having 17972.38 MJ-mm/ha/h/yr average R-factor value while Leh (Ladakh) district is least vulnerable with lowest (42.12 MJ-mm/ha/h/yr) rainfall erosivity factor. A total of 265 districts have average R-factor values greater than the national average rainfall erosivity factor (1200 MJ-mm/ha/h/yr). Only 20 districts in India are there having average rainfall erosivity values greater than 7000 MJ-mm/ha/h/yr, in which all districts lie in the Assam & Meghalaya sub-division of IMD except Jalpaiguri district of West Bengal sub-division having 9848.98 MJ-mm/ha/h/yr average R-factor value.

3.2. FI and MFI estimation

The results are shown in Fig. 6(a) to 6(f). Calculated MFI values with all the three datasets were compared with the Tiwari et al., (2016) study and found that the MFI values calculated using CHIRPS daily rainfall product produced better correlation (Pearson correlation 0.60). These two datasets were also plotted on x-y axes in scattered way corresponding to the 52 rain-gauge stations (Fig. 10).

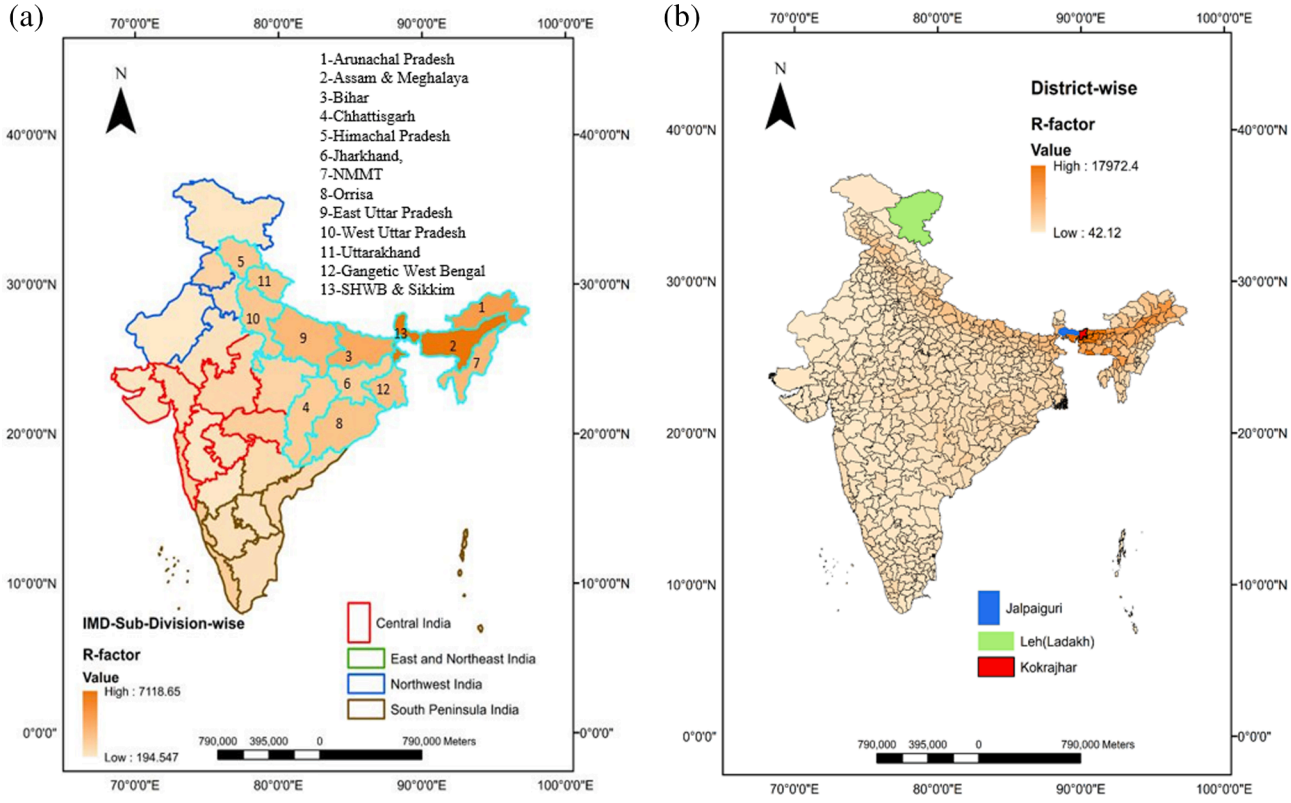

Fig. 5. (a) and (b) Spatial distribution of average R-factor values in IMD sub-divisions as well as districts of India.

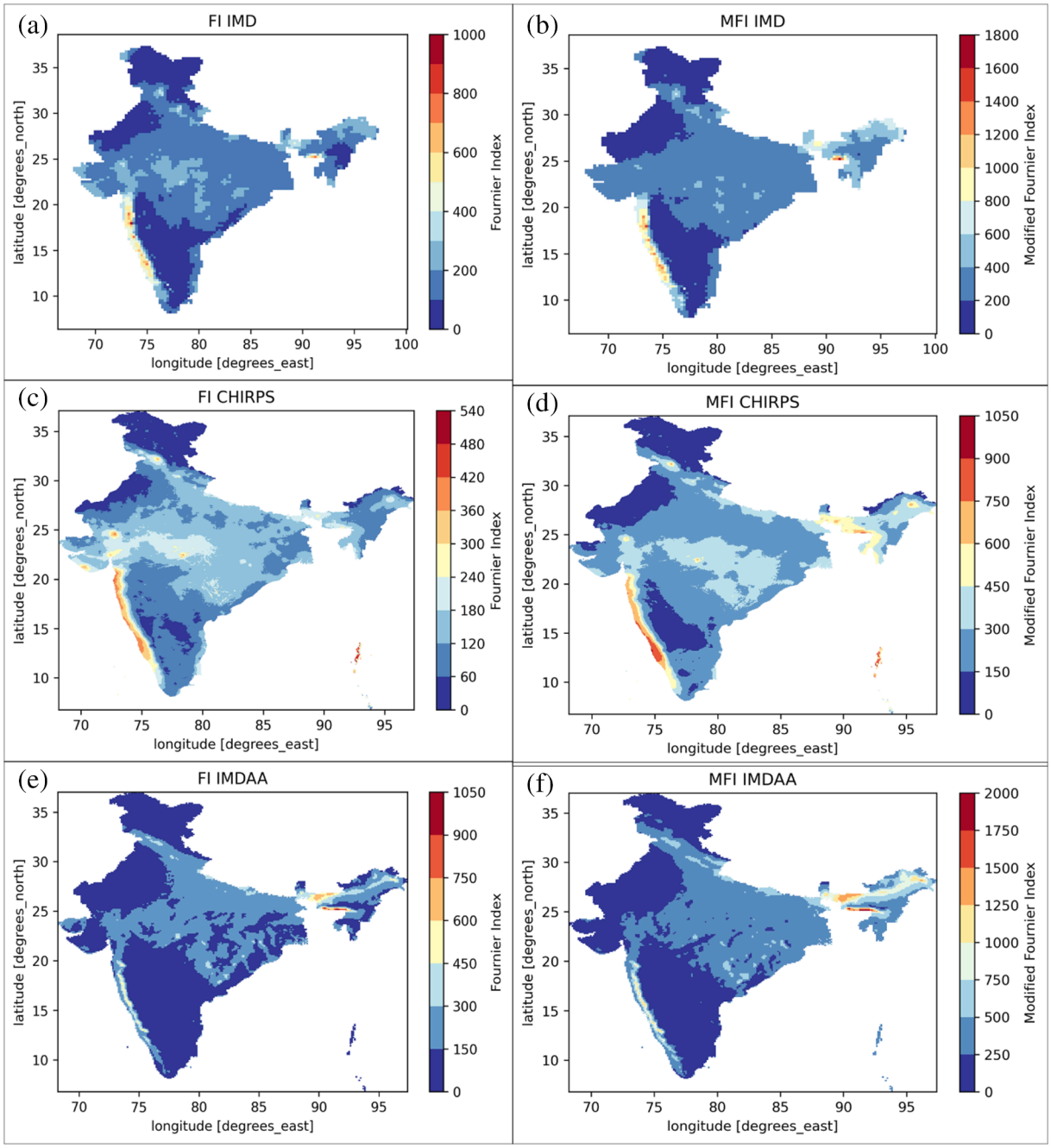

Fig. 6. (a) to 6(f) FI and MFI indices over India using IMD daily, CHIRPS daily and IMDAA hourly precipitation datasets over India.

Table 4
Erosive class table for India depending upon FI and MFI (Lukić et al., 2019).

Erosive Class	FI	Percentage (%)	Erosive Class	MFI	Percentage (%)
Very low	0–20	0	Very low	0–60	0
Low	20–40	0.03	Low	60–90	0.39
Moderate	40–60	3.51	Moderate	90–120	3.95
Severe	60–80	13.88	High	120–160	15.67
Very severe	80–100	11.89	Very high	>160	79.98
Extremely Severe	>100	70.69			

Analyzing FI and MFI maps resultant from all the three datasets, it was observed that the spatial distribution of the values (FI and MFI both) did not have the same trend. Temporal-spatial average values estimated of FI were of similar range (0.35, 0.33 and 0.33 respectively) but MFI values were of different range over India i.e., 283.77, 243.96 and 287.62 respectively using IMD daily, CHIRPS daily and IMDAA hourly rainfall datasets. Differences were also spotted in the spatially maximum and minimum values of MFI, maximum as 1637.88, 977.95 and 1911.31, and minimum as 78.57, 10.39 and 17.8 respectively for IMD daily, CHIRPS daily and IMDAA hourly precipitation datasets. An erosive classification was also performed base on FI and MFI ranges (Lukić et al., 2019). The outcome of this analysis was explained in the Table 4. Considering FI values, more than 70% of the values referring to extremely severe erosive class while 0.03% values refer to low and very low erosive classes. About 96% of the MFI values referring to very high and high erosive classes while only 0.39% values come under low and very low erosive classes.

These six maps of FI and MFI Fig. 6(a)–(f) and the R-factor map Fig. 2

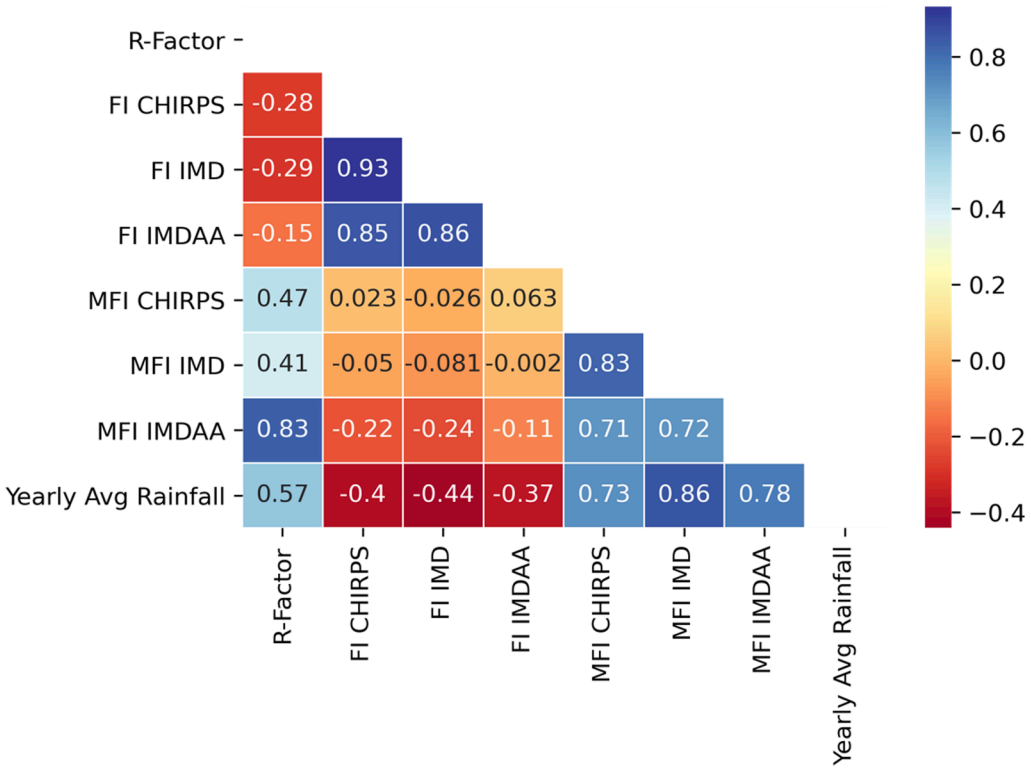

Fig. 7. Correlations among R-factor, FI, MFI and yearly average precipitation.

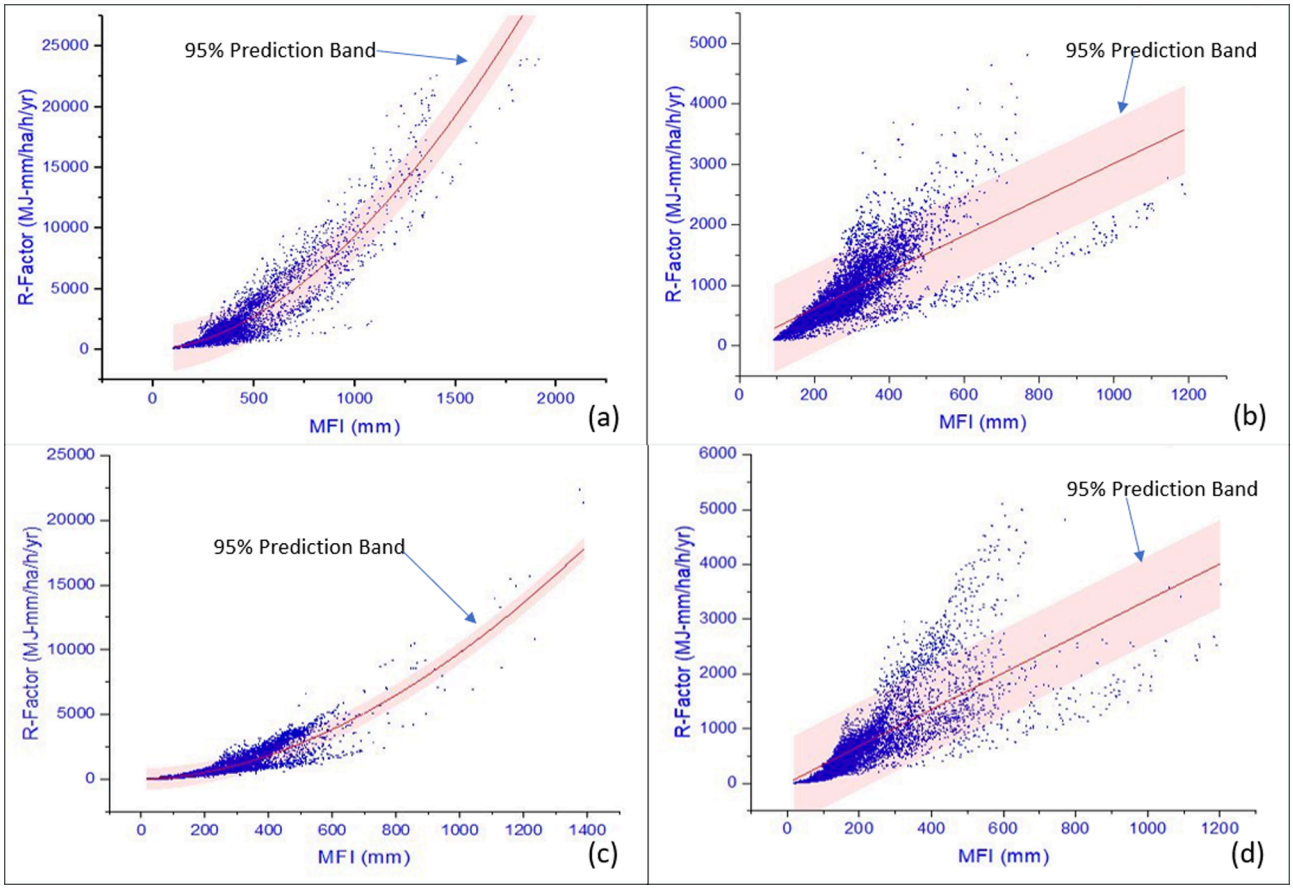

Fig. 8. Relation between R-factors (MJ-mm/ha/h/yr) and Modified Fournier Index (MFI) based on IMDAA hourly data for 1979–2019 for East & Northeast, Central, Northwest, and South Peninsula regions defined by IMD (n = 171484).

Table 5
Regression equation for R-factor for each region of IMD.

Sr No	IMD Regions	α	β	r2	Error in α	Error in β
1	Central India	3.371	0.984	0.56	0.0761	0.004
2	East and Northeast India	0.041	1.785	0.89	7.80 e^-04	0.003
3	Northwest India	0.033	1.826	0.81	8.19 e^-04	0.004
4	South Peninsula India	3.618	0.989	0.62	0.0738	0.003

(b) were further processed to check the sensitivity of these indices with rainfall erosivity factor over India. These maps were also analyzed with the temporal yearly average (1901–2019) of IMD daily rainfall data to check the relationship with it. Similar type of methodology was adopted in this case as it was in previous section for intercorrelation analysis among R-factor maps using different types of equation (equation 1 to 6). On average 171,484 values were extracted at 0.044° arc distance (~5 km) interval for each map throughout the nation and Pearson correlation was then correlated for each parameter. The result of the correlation analysis is shown in Fig. 7 in the form of a heatmap.

From Fig. 7, it is clearly visible that MFI estimated using IMDAA hourly precipitation dataset is highly correlated (Pearson correlation 0.83) with rainfall erosivity in Indian context. Long term (119 years) temporal average yearly precipitation values are also showing higher correlations (0.86, 0.78 and 0.73) with MFI calculated using IMD daily, IMDAA hourly and CHIRPS daily rainfall datasets. Fournier index estimations using all the three datasets have lowest negative correlation coefficients (-0.15, −0.28 and −0.29) with R-factor values over the nation.

Modified Fournier Index estimated using IMDAA daily data (MFI_IMDAA) values were further plotted with the R-factor values to get best-fit empirical equation for calculating rainfall erosivity factor using MFI over India (Fig. 8 (a) to (d)). Considering variation in climate conditions of the nation, four equations were suggested to estimate rainfall erosivity factor with the help of MFI for each regions defined by IMD (Central, East and North-east, North-west, and Peninsula India) in the form of a simple power-law formula ($R = \alpha\ MFI\hat{}\beta$), where R is the rainfall erosivity in (MJ-mm/ha/h/yr), MFI is in (mm), β is the law's exponent and α is a constant. α and β for each region are determined by plotting R v/s MFI plot on y-axis and x-axis respectively in scattered manner to get the best fit curve. The details of these regression equations are mentioned in Table 5. The separate plots of the R-factor with corresponding MFI values was shown for each IMD region in Fig. 8(a) to (d) with 95% prediction band.

4. Uncertainty and limitations

The approach followed in this study consists of application of hourly (I60) precipitation intensity data for the calculation of rainfall erosivity factor. R-factor is defined as the product of total kinetic energy by the maximum 30-minutes rainfall intensity for an erosive rainfall event (Vantas et al., 2019). This study utilized some of best-available high-resolution rainfall datasets for entire Indian region, these gridded datasets have their own limitations depending upon the source and mode of its derivation and the intrinsic differences in spatial scales (Shen et al., 2010; Tapiador et al., 2012). In the future, radar-based sub-hourly rainfall retrievals could be used to estimate rainfall erosivity.

5. 4. Conclusions and recommendations

This study describes the variation of rainfall erosivity pattern throughout the nation and check the applicability of alternative indices to estimate R-factor in Indian context. High resolution rainfall (IMDAA hourly reanalysis product) for 40 years and daily rainfall data (IMD daily and CHIRPS daily) for 116 years and 39 years respectively were used for the study. The main conclusions of this research are as follows:

All the six equations to calculate R-factor are applicable throughout the national region, as the Pearson's correlation coefficients for each equation was greater than 0.98. Hence, any of the six methods could be used to calculate rainfall erosivity over India.

The average R-factor value estimated for India is 1200 MJ-mm/ha/h/yr, while maximum value spotted was 23909.21 MJ-mm/ha/h/yr in the Laitknsew and Cherrapunji region of East Khasi Hills in Meghalaya state, and minimum value in the Shahi Kangri mountain region of Ladakh area as 8.10 MJ-mm/ha/h/yr. Kokrajhar district of Assam & Meghalaya sub-division is more vulnerable to rainfall erosivity having 17972.38 MJ-mm/ha/h/yr average R-factor value while Leh (Ladakh) district is least vulnerable with lowest (42.12 MJ-mm/ha/h/yr) rainfall erosivity factor.

About 71.2% of the total point values taken into analysis are less than average value of R-factor (1200 MJ-mm/ha/h/yr). Only 1.95% R-values estimated were greater than 7000 MJ-mm/ha/h/yr and 0.5% values greater than 13000 MJ-mm/ha/h/yr.

MFI (Modified Fourier Index) is highly correlated to the rainfall erosivity throughout the Indian region with a Pearson's correlation coefficient of 0.83. Hence, it was recommended that MFI should be preferably used to estimate rainfall erosivity in absence of high-resolution precipitation product in Indian context.

Four power law equations ($R = \alpha*MFI\hat{}\beta$) were also recommended to estimate rainfall erosivity with the help of MFI in the absence of high-resolution precipitation datasets as an alternative method to estimate rainfall erosivity for each region identified by IMD.

This is the first national-scale assessment of rainfall erosivity over India using gridded precipitation, which will be helpful for agricultural experts, watershed managers, agronomists, and soil-conservational experts to apply this rainfall erosivity map of the country as an additional database for incorporating safety measures to minimize soil erosion.

Declaration of Competing Interest

The authors declare that they have no known competing financial interests or personal relationships that could have appeared to influence the work reported in this paper.

Acknowledgements

This work was supported by Indian Space Research Organization (RP04139), IITD-UCL MFIRP (MI02273), and the IIT Delhi New Faculty Seed Grant. Authors gratefully acknowledge the India Meteorological Department (IMD) and NCMRWF, Ministry of Earth Sciences, Government of India for providing access to the datasets. The authors would also like to thank the handling editor and the anonymous reviewers for providing useful comments which greatly improved the quality of this manuscript.

References

Abram, N.J., Gagan, M.K., Cole, J.E., Hantoro, W.S., Mudelsee, M., 2008. Recent intensification of tropical climate variability in the Indian Ocean. Nat. Geosci. 1 (12), 849–853. https://doi.org/10.1038/ngeo357.

Arnoldus, H.M.J., 1977. Methodology used to determine the maximum potential average annual soil loss due to sheet and rill erosion in Morocco.

Becker, A., Finger, P., Meyer-Christoffer, A., Rudolf, B., Schamm, K., Schneider, U., Ziese, M., 2013. A description of the global land-surface precipitation data products of the Global Precipitation Climatology Centre with sample applications including centennial (trend) analysis from 1901–present. Earth Syst. Sci. Data 5 (1), 71–99.

Bosco, C., De Rigo, D., Dewitte, O., Poesen, J., Panagos, P., 2015. Modelling soil erosion at European scale: Towards harmonization and reproducibility. Nat. Hazards Earth Syst. Sci. 15, 225–245. https://doi.org/10.5194/nhess-15-225-2015.

Brown, L.C., Foster, G.R., 1987. storm Erosivity Using Idealized Intensity Distributions Distributions 67, 379–386.

Bryan, R.B., 2000. Soil erodibility and processes of water erosion on hillslope. Geomorphology 32 (3-4), 385–415. https://doi.org/10.1016/S0169-555X(99)00105-1.

Capolongo, D., Diodato, N., Mannaerts, C.M., Piccarreta, M., Strobl, R.O., 2008. Analyzing temporal changes in climate erosivity using a simplified rainfall erosivity model in Basilicata (southern Italy). J. Hydrol. 356 (1-2), 119–130. https://doi.org/10.1016/j.jhydrol.2008.04.002.

Catari, G., Latron, J., Gallart, F., 2011. Assessing the sources of uncertainty associated with the calculation of rainfall kinetic energy and erosivity - application to the Upper Llobregat Basin. NE Spain. Hydrol. Earth Syst. Sci. 15, 679–688. https://doi.org/10.5194/hess-15-679-2011.

Chen, M., Shi, W., Xie, P., Silva, V.B.S., Kousky, V.E., Wayne Higgins, R., Janowiak, J.E., 2008. Assessing objective techniques for gauge-based analyses of global daily precipitation. J. Geophys. Res. Atmos. 113 (D4) https://doi.org/10.1029/2007JD009132.

Dabral, P.P., Baithuri, N., Pandey, A., 2008. Soil erosion assessment in a hilly catchment of North Eastern India using USLE, GIS and remote sensing. Water Resour. Manage. 22 (12), 1783–1798. https://doi.org/10.1007/s11269-008-9253-9.

Dash, C.J., Adhikary, P.P., Das, N.K., Alam, N.M., Mandal, U., Mishra, P.K., 2018. Comparison of rainfall kinetic energy–intensity relationships for Eastern Ghats Highland region of India. Nat. Hazards 93 (1), 547–558. https://doi.org/10.1007/s11069-018-3314-z.

Dash, C.J., Das, N.K., Adhikary, P.P., 2019. Rainfall erosivity and erosivity density in Eastern Ghats. Nat. Hazards 97, 727–746. https://doi.org/10.1007/s11069-019-03670-9.

Davies, T., Cullen, M.J.P., Malcolm, A.J., Mawson, M.H., Staniforth, A., White, A.A., Wood, N., 2005. A new dynamical core for the Met Office's global and regional modelling of the atmosphere. Q. J. R. Meteorol. Soc. A J. Atmos. Sci. Appl. Meteorol. Phys. Oceanogr. 131 (608), 1759–1782.

Diodato, N., 2004. Estimating RUSLE's rainfall factor in the part of Italy with a Mediterranean rainfall regime. Hydrol. Earth Syst. Sci. 8, 103–107. https://doi.org/10.5194/hess-8-103-2004.

FAO, 1977. Assessing Soil Degradation, 34th ed. FAO Soils Bulletin.

Fornis, R.L., Vermeulen, H.R., Nieuwenhuis, J.D., 2005. Kinetic energy-rainfall intensity relationship for Central Cebu, Philippines for soil erosion studies. J. Hydrol. 300 (1-4), 20–32. https://doi.org/10.1016/j.jhydrol.2004.04.027.

Fournier, F., 1960. Climat et erosion. Presses universitaires de France Paris.

Funk, C., Peterson, P., Landsfeld, M., Pedreros, D., Verdin, J., Shukla, S., Husak, G., Rowland, J., Harrison, L., Hoell, A., Michaelsen, J., 2015. The climate hazards infrared precipitation with stations—a new environmental record for monitoring extremes. Sci Data 2 (1). https://doi.org/10.1038/sdata.2015.66.

Harris, I., Jones, P.D., Osborn, T.J., Lister, D.H., 2014. Updated high-resolution grids of monthly climatic observations - the CRU TS3.10 Dataset. Int. J. Climatol. 34 (3), 623–642. https://doi.org/10.1002/joc.3711.

Hartmann, D.L., Michelsen, M.L., 1989. Intraseasonal periodicities in Indian rainfall. J. Atmos. Sci. 46 (18), 2838–2862.

Hudson, N.W., 1961. An introduction to the mechanics of soil erosion under conditions of subtropical rainfall. Proc. Trans. Rhod. Sci. Assoc 49, 14–25.

Huffman, G.J., Adler, R.F., Bolvin, D.T., Gu, G., Nelkin, E.J., Bowman, K.P., Hong, Y., Stocker, E.F., Wolff, D.B., 2007. The TRMM Multisatellite Precipitation Analysis (TMPA): Quasi-global, multiyear, combined-sensor precipitation estimates at fine scales. J. Hydrometeorol. 8, 38–55. https://doi.org/10.1175/JHM560.1.

Indirarani, S., Arulalan, T., George, J.P., Rajagopal, E.N., Renshaw, R., Maycock, A., Barker, D.M., Rajeevan, M., 2021. IMDAA: High-resolution satellite-era reanalysis for the Indian monsoon region. J. Clim. 34, 5109–5133. https://doi.org/10.1175/JCLI-D-20-0412.1.

Kidd, C., Huffman, G., 2011. Global precipitation measurement. Meteorol. Appl. 18, 334–353. https://doi.org/10.1002/met.284.

Kotlarski, S., Szabó, P., Herrera, S., Räty, O., Keuler, K., Soares, P.M., Cardoso, R.M., Bosshard, T., Pagé, C., Boberg, F., Gutiérrez, J.M., Isotta, F.A., Jaczewski, A., Kreienkamp, F., Liniger, M.A., Lussana, C., Pianko-Kluczyńska, K., 2019. Observational uncertainty and regional climate model evaluation: a pan-European perspective. Int. J. Climatol. https://doi.org/10.1002/joc.5249.

Krishnamurthy, V., Shukla, J., 2008. Seasonal persistence and propagation of intraseasonal patterns over the Indian monsoon region. Clim. Dyn. 30 (4), 353–369. https://doi.org/10.1007/s00382-007-0300-7.

Krishnamurthy, V., Shukla, J., 2007. Intraseasonal and seasonally persisting patterns of Indian monsoon rainfall. J. Clim. 20, 3–20. https://doi.org/10.1175/JCLI3981.1.

Krishnamurthy, V., Shukla, J., 2000. Intraseasonal and interannual variability of rainfall over India. J. Clim. 13 (24), 4366–4377.

Lobo, G.P., Bonilla, C.A., 2015. Sensitivity analysis of kinetic energy-intensity relationships and maximum rainfall intensities on rainfall erosivity using a long-term precipitation dataset. J. Hydrol. 527, 788–793. https://doi.org/10.1016/j.jhydrol.2015.05.045.

Love, T.B., Kumar, V., Xie, P.P., Thiaw, W., 2004. A 20-year daily Africa precipitation climatology using satellite and gauge data. Bull. Am. Meteorol. Soc. 5213–5216.

Lukić, T., Bjelajac, D., Fitzsimmons, K.E., Marković, S.B., Basarin, B., Mlađan, D., Micić, T., Schaetzl, R.J., Gavrilov, M.B., Milanović, M., Sipos, G., Mezősi, G., Knežević-Lukić, N., Milinčić, M., Létal, A., Samardžić, I., 2018. Factors triggering landslide occurrence on the Zemun loess plateau, Belgrade area, Serbia. Environ. Earth Sci. 77 (13) https://doi.org/10.1007/s12665-018-7712-z.

Lukić, T., Leščešen, I., Sakulski, D., Basarin, B., Jordaan, A., 2016. Rainfall erosivity as an indicator of sliding occurrence along the southern slopes of the bačka loess plateau: A case study of the kula settlement, vojvodina (North Serbia). Carpathian J. Earth Environ. Sci. 11, 303–318.

Lukić, T., Lukić, A., Basarin, B., Ponjiger, T.M., Blagojević, D., Mesaroš, M., Milanović, M., Gavrilov, M., Pavić, D., Zorn, M., Komac, B., Miljković, D., Sakulski, D., Babić-Kekez, S., Morar, C., Janićević, S., 2019. Rainfall erosivity and extreme precipitation in the Pannonian basin. Open Geosci. 11, 664–681. https://doi.org/10.1515/geo-2019-0053.

Maidment, R.I., Grimes, D., Allan, R.P., Tarnavsky, E., Stringer, M., Hewison, T., Roebeling, R., Black, E., 2014. The 30 year TAMSAT African Rainfall Climatology And Time series (TARCAT) data set. J. Geophys. Res. Atmos. 119 (18) https://doi.org/10.1002/jgrd.v119.1810.1002/2014JD021927.

McGregor, K.C., Bingner, R.L., Bowie, A.J., Foster, G.R., 1995. Erosivity index values for northern Mississippi. Trans. - Am. Soc. Agric. Eng. 38, 1039–1047. 10.13031/2013.27921.

Meshesha, D.T., Tsunekawa, A., Tsubo, M., Haregeweyn, N., Tegegne, F., 2016. Evaluation of kinetic energy and erosivity potential of simulated rainfall using Laser Precipitation Monitor. Catena 137, 237–243. 10.1016/j.catena.2015.09.017.

Morar, C., Lukić, T., Basarin, B., Valjarević, A., Vujičić, M., Niemets, L., Telebienieva, I., Boros, L., Nagy, G., 2021. Shaping sustainable urban environments by addressing the hydro-meteorological factors in landslide occurrence: ciuperca hill (Oradea, romania). Int. J. Environ. Res. Public Health 18 (9), 5022. https://doi.org/10.3390/ijerph18095022.

Nazzareno, D., Luigi, G., Paola, R., Gerardo, G., Maria, G.F., 2015. Spatial Pattern of Hydrological Predictability of Landslide-Prone Areas. In: Lollino, G., Giordan, D., Crosta, G.B., Corominas, J., Azzam, R., Wasowski, J., Sciarra, N. (Eds.), Engineering Geology for Society and Territory - Volume 2. Springer International Publishing, Cham, pp. 1611–1613. https://doi.org/10.1007/978-3-319-09057-3_286.

New, M., Hulme, M., Jones, P., 1999. Representing Twentieth-Century Space – Time Climate Variability. Part I: Development of a 1961–90 Mean Monthly Terrestrial Climatology. J. Clim. 12 (3), 829–856.

New, M., Todd, M., Hulme, M., Jones, P., 2001. Precipitation Measurements and Trends in the. Int. J. Climatol. 1922, 1899–1922.

Padulano, R., Rianna, G., Santini, M., 2021. Datasets and approaches for the estimation of rainfall erosivity over Italy: a comprehensive comparison study and a new method. J. Hydrol. Reg. Stud. 34, 100788. https://doi.org/10.1016/j.ejrh.2021.100788.

Pai, D.S., Sridhar, L., Rajeevan, M., Sreejith, O.P., Satbhai, N.S., Mukhopadyay, B., 2014. Development of a new high spatial resolution (0 . 25 ° × 0 . 25 °) Long Period (1901-2010) daily gridded rainfall data set over India and its comparison with existing data sets over the region data sets of different spatial resolutions and time period 1, 1–18.

Panagos, P., Ballabio, C., Borrelli, P., Meusburger, K., Klik, A., Rousseva, S., Tadić, M.P., Michaelides, S., Hrabalíková, M., Olsen, P., Aalto, J., Lakatos, M., Rymszewicz, A., Dumitrescu, A., Beguería, S., Alewell, C., 2015a. Rainfall erosivity in Europe. Sci. Total Environ. 511, 801–814. 10.1016/j.scitotenv.2015.01.008.

Panagos, P., Borrelli, P., Meusburger, K., Yu, B., Klik, A., Lim, K.J., Yang, J.E., Ni, J., Miao, C., Chattopadhyay, N., Sadeghi, S.H., Hazbavi, Z., Zabihi, M., Larionov, G.A., Krasnov, S.F., Gorobets, A. V., Levi, Y., Erpul, G., Birkel, C., Hoyos, N., Naipal, V., Oliveira, P.T.S., Bonilla, C.A., Meddi, M., Nel, W., Al Dashti, H., Boni, M., Diodato, N., Van Oost, K., Nearing, M., Ballabio, C., 2017. Global rainfall erosivity assessment based on high-temporal resolution rainfall records. Sci. Rep. 7, 1–12. 10.1038/s41598-017-04282-8.

Panagos, P., Borrelli, P., Poesen, J., Ballabio, C., Lugato, E., Meusburger, K., Montanarella, L., Alewell, C., 2015b. The new assessment of soil loss by water erosion in Europe. Environ. Sci. Policy 54, 438–447. https://doi.org/10.1016/j.envsci.2015.08.012.

Pandey, A., Chowdary, V.M., Mal, B.C., 2007. Identification of critical erosion prone areas in the small agricultural watershed using USLE, GIS and remote sensing. Water Resour. Manag. 21 (4), 729–746. https://doi.org/10.1007/s11269-006-9061-z.

Prasannakumar, V., Shiny, R., Geetha, N., Vijith, H., 2011. Spatial prediction of soil erosion risk by remote sensing, GIS and RUSLE approach: A case study of Siruvani river watershed in Attapady valley, Kerala, India. Environ. Earth Sci. 64 (4), 965–972. https://doi.org/10.1007/s12665-011-0913-3.

Prasannakumar, V., Vijith, H., Abinod, S., Geetha, N., 2012. Estimation of soil erosion risk within a small mountainous sub-watershed in Kerala, India, using Revised Universal Soil Loss Equation (RUSLE) and geo-information technology. Geosci. Front. 3 (2), 209–215. https://doi.org/10.1016/j.gsf.2011.11.003.

Rajbanshi, J., Bhattacharya, S., 2020. Assessment of soil erosion, sediment yield and basin specific controlling factors using RUSLE-SDR and PLSR approach in Konar river basin. India. J. Hydrol. 587, 124935. https://doi.org/10.1016/j.jhydrol.2020.124935.

Rawat, J.S., Joshi, R.C., Mesia, M., 2013. Estimation of erosivity index and soil loss under different land uses in the tropical foothills of Eastern Himalaya (India). Trop. Ecol. 54, 47–58.

Rawlins, F., Ballard, S.P., Bovis, K.J., Clayton, A.M., Li, D., Inverarity, G.W., Lorenc, A.C., Payne, T.J., 2007. The met office global four-dimensional variational data assimilation scheme. Q. J. R. Meteorol. Soc. 133 (623), 347–362. https://doi.org/10.1002/qj.32.

Renard, K., Foster, G. R., Weesies, G. A., McCool, D. K., Yoder, D. C., Coordinators, 1997. Predicting Soil Erosion by Water: A Guide to Conser vation Planning With the Revised Universal Soil Loss Equation (RUSLE), U .S. Department of Agriculture, Agriculture Handbook No. 703.

Renard, K.G., Foster, G.R., Weesies, G.A., Porter, J.P., 1991. RUSLE: revised universal soil loss equation. J. Soil Water Conserv. 46, 30–33.

Renard, K.G., Freimund, J.R., 1994. Using monthly precipitation data to estimate the R-factor in the revised USLE. J. Hydrol. 157 (1-4), 287–306.

Renard, K.G., Laflen, J.M., Foster, G.R., McCool, D.K., 1994. The revised universal soil loss equation. Soil Eros. Res. methods 2, 105–124.

Rosewell, 1986. Rainfall kinetic energy in eastern Australia. J. Mater. Process. Technol. 1, 1–8.

Schneider, U., Becker, A., Finger, P., Meyer-Christoffer, A., Ziese, M., Rudolf, B., 2014. GPCC's new land surface precipitation climatology based on quality-controlled in

situ data and its role in quantifying the global water cycle. Theor. Appl. Climatol. 115 (1-2), 15–40.
Sharifah, M.S., Sabry, A., Jaafar, O., 2006. Rainsplash erosion: A case study in Tekala River Catchment, East Selangor Malaysia. Geogr. Malaysian J. Soc. Sp. 2, 43–57.
Shen, Y., Feng, M., Zhang, H., Gao, F., 2010. Interpolation methods of China daily precipitation data [J]. J. Appl. Meteorol. Sci. 21, 279–286.
Sinzot, A., Bollinne, A., Laurant, A., Erpicum, M., Pissart, A., 1989. A contribution to the development of an erosivity index adapted to the prediction of erosion in Belgium. Earth Surf. Process. Landforms 14 (6), 509–515.
Tapiador, F.J., Turk, F.J., Petersen, W., Hou, A.Y., García-Ortega, E., Machado, L.A.T., Angelis, C.F., Salio, P., Kidd, C., Huffman, G.J., de Castro, M., 2012. Global precipitation measurement: Methods, datasets and applications. Atmos. Res. 104–105, 70–97. https://doi.org/10.1016/j.atmosres.2011.10.021.
Tarnavsky, E., Grimes, D., Maidment, R., Black, E., Allan, R.P., Stringer, M., Chadwick, R., Kayitakire, F., 2014. Extension of the TAMSAT satellite-based rainfall monitoring over Africa and from 1983 to present. J. Appl. Meteorol. Climatol. 53, 2805–2822. https://doi.org/10.1175/JAMC-D-14-0016.1.
Titchner, H.A., Rayner, N.A., 2014. The Met Office Hadley Centre sea ice and sea surface temperature data set, version 2: 1. Sea ice concentrations. J. Geophys. Res. Atmos. 119 (6), 2864–2889.
Tiwari, H., Rai, S.P., Kumar, D., Sharma, N., 2016. Rainfall erosivity factor for India using modified Fourier index. J. Appl. Water Eng. Res. 4 (2), 83–91. https://doi.org/10.1080/23249676.2015.1064038.
Tripathi, R.P., Singh, H.P., 1993. Soil erosion and conservation. Wiley Eastern Limited.
Usón, A., Ramos, M.C., 2001. An improved rainfall erosivity index obtained from experimental interrill soil losses in soils with a mediterranean climate. Catena 43 (4), 293–305. https://doi.org/10.1016/S0341-8162(00)00150-8.
van Dijk, A.I.J.M., Bruijnzeel, L.A., Rosewell, C.J., 2002. Rainfall intensity-kinetic energy relationships: A critical literature appraisal. J. Hydrol. 261 (1-4), 1–23. https://doi.org/10.1016/S0022-1694(02)00020-3.
Vantas, K., Sidiropoulos, E., Evangelides, C., 2019. Rainfall erosivity and its estimation: Conventional and machine learning methods. Soil Erosion-Rainfall Erosivity Risk Assess. 19.
Villarini, G., Krajewski, W.F., 2008. Empirically-based modeling of spatial sampling uncertainties associated with rainfall measurements by rain gauges. Adv. Water Resour. 31 (7), 1015–1023. https://doi.org/10.1016/j.advwatres.2008.04.007.
Vrieling, A., Sterk, G., de Jong, S.M., 2010. Satellite-based estimation of rainfall erosivity for Africa. J. Hydrol. 395 (3-4), 235–241. https://doi.org/10.1016/j.jhydrol.2010.10.035.
Williams, R.G., Sheridan, J.M., 1991. Depth Resolution on Ei Calculation 402–406.
Willmott, C.J., Matsuura, K., 2009. Terrestrial precipitation: 1900–2008 gridded monthly time series. Cent. Clim. Res. Dep. Geogr. Cent. Clim. Res. Univ. Delaware.
Willmott, C.J., Matsuura, K., 1995. Smart interpolation of annually averaged air temperature in the United States. J. Appl. Meteorol. Climatol. 34 (12), 2577–2586.
Willmott, C.J., Robeson, S.M., 1995. Climatologically aided interpolation (CAI) of terrestrial air temperature. Int. J. Climatol. 15 (2), 221–229.
Wischmeier, W.H., 1959. A rainfall erosion index for a universal soil-loss equation. Soil Sci. Soc. Am. J. 23 (3), 246–249. https://doi.org/10.2136/sssaj1959.03615995002300030027x.
Wischmeier, W.H., Smith, D.D., 1978. Predicting rainfall erosion losses: a guide to conservation planning. Department of Agriculture, Science and Education Administration.
Wischmeier, W.H., Smith, D.D., 1958. Rainfall energy and its relationship to soil loss. Eos. Trans. Am. Geophys. Union 39 (2), 285. https://doi.org/10.1029/TR039i002p00285.
Xie, P., Arkin, P.A., 1997. Global precipitation: a 17-year monthly analysis based on gauge observations, satellite estimates, and numerical model outputs. Bull. Am. Meteorol. Soc. 78 (11), 2539–2558.
Xie, P., Yatagai, A., Chen, M., Hayasaka, T., Fukushima, Y., Liu, C., Yang, S., 2007. A gauge-based analysis of daily precipitation over East Asia. J. Hydrometeorol. 8, 607–626. https://doi.org/10.1175/JHM583.1.
Zheng, M., Chen, X., 2015. Statistical determination of rainfall-runoff erosivity indices for single storms in the Chinese Loess Plateau. PLoS One 10, 1–18. 10.1371/journal.pone.0117989.